

NEAR-FIELD ACOUSTIC HOLOGRAPHY AND NON-NEGATIVE INTENSITY FOR PREDICTION OF SOUND RADIATION

Daipei Liu¹, Zdeněk Havránek², Herwig Peters¹, Steffen Marburg³, Nicole Kessissoglou¹

¹School of Mechanical and Manufacturing Engineering
UNSW Australia, Sydney, NSW 2052, Australia
Email: daipei.liu@unsw.edu.au

²Department of Control and Instrumentation
Brno University of Technology, Technická 3082/12, Brno, Czech Republic
Email: havranek@feec.vutbr.cz

³Vibroacoustics of Vehicles and Machines
Technische Universität München
Boltzmann Str. 15, 85748 Garching, München, Germany
Email: steffen.marburg@tum.de

Abstract

In this work, near-field acoustic holography and non-negative intensity methods are used to predict the radiated sound of a vibrating structure. Near-field acoustic holography (NAH) is an experimental technique to reconstruct the acoustic field on the surface of the structure. The sound pressure field was measured using a microphone array close to the structural surface. The normal velocity of the plate was also measured. Supersonic intensity was calculated using experimental data based on the NAH measurements. Non-negative intensity is a quantity which allows the surface contributions of a vibrating structure to the radiated sound based on acoustic radiation modes to be predicted. An example of a point driven plate is used to compare these two source localization techniques. Results show that both techniques are successful in predicting the sound radiation patterns and yield similar results for all frequencies considered.

1. Introduction

Prediction of radiated sound from vibrating structures is required for structural design optimization and effective noise control [1, 2, 3]. There are a number of techniques to predict exterior radiated sound from vibrating structures, including analytical, numerical and experimental methods. Near-field acoustic holography (NAH) is an experimental technique introduced by Williams and Maynard [4] to reconstruct the acoustic pressure, normal velocity and intensity on the surface of a radiating object, using microphone measurements over a two-dimensional surface in the acoustic near field and data processing. Digital NAH [5], generalized NAH [6] and boundary element method based NAH [7] were developed to reconstruct the acoustic field using analytical and numerical algorithms. In order to reduce the computational cost for large complex structures, patch NAH [8, 9] and equivalent source method based NAH [10, 11] were developed to significantly speed up the computation time.

Williams [12, 13] introduced the concept of supersonic acoustic intensity (SSI) to identify wave components of the sound field propagating to the far field. The acoustic field was measured and reconstructed using NAH. After filtering out the subsonic wave components of the vibrating structure that only generate evanescent waves in the near field, the remaining supersonic components that radiate to the far field were identified. Supersonic acoustic intensity has also been used to examine arbitrarily shaped geometries [14, 15, 16, 17].

Another numerical method to identify the surface areas of a vibrating structure that radiate far-field sound is the surface contribution method [18], which yields a non-negative intensity (NNI). The NNI is based on acoustic radiation modes, acoustic radiation efficiency and either the acoustic pressure or normal structural velocity at the surface of a vibrating structure. In contrast to SSI which has areas of both negative and positive intensity, NNI is always positive and thus avoids any cancellation effects. Williams [19] developed a method to obtain non-negative intensity using convolution formulations that require only the pressure or the structural velocity field. The non-negative intensity of a point driven plate was compared to results obtained using supersonic intensity, also developed by Williams [12, 13], showing good agreement.

In this paper, supersonic acoustic intensity and non-negative intensity are used to identify the locations (hot spots) on the surface of a vibrating structure that significantly contribute to radiated sound. Supersonic intensity is calculated using experimental data based on NAH measurements and NNI is calculated based on data computed by the boundary element method. An example of a point driven plate is used to compare these two source localization techniques. Results show that both techniques are successful in predicting sound radiation patterns and yield similar results for all frequencies considered here.

2. Numerical Method

Complex sound intensity on a structural surface can be separated into its active and reactive components [19]. The active component is the energy radiated to the far field, while the reactive component only contributes to instantaneous power radiation that vanishes when averaged over a period of time. The active acoustic intensity is defined by

$$\mathbf{I} = \frac{1}{2} \Re \{ \mathbf{p} \mathbf{v}^* \} \quad (1)$$

where \mathbf{p} and \mathbf{v} are respectively the acoustic pressure and the particle velocity calculated using a fully coupled finite element/boundary element approach. $()^*$ denotes the complex conjugate. The radiated sound power is defined as [20]

$$P = \int_{\Gamma} \mathbf{I} \cdot \mathbf{n} \, d\Gamma \quad (2)$$

where Γ is the boundary of the exterior acoustic domain and \mathbf{n} is the normal direction on Γ .

The non-negative intensity is always positive. To achieve this, the radiated sound power is expressed as [18]

$$P = \frac{1}{2} \int_{\Gamma} \beta(\mathbf{x}) \beta^*(\mathbf{x}) \, d\Gamma(\mathbf{x}) \quad (3)$$

where $\beta(\mathbf{x})$ is a quantity without physical significance and can be computed using acoustic radiation modes and the surface velocity of the vibrating surface [18]. The non-negative intensity (NNI) is defined as

$$I^{\text{NNI}}(\mathbf{x}) = \frac{1}{2} \beta(\mathbf{x}) \beta^*(\mathbf{x}) \quad (4)$$

3. Experimental Method

Near-field acoustic holography (NAH) is an experimental technique to reconstruct the sound pressure on the surface of a vibrating structure. It is usually assumed that there are sources only on one side of the measurement plane. Based on the sound pressure measured on the hologram plane $p_m(x_h, y_h, z_h)$, the

experimentally predicted sound pressure on the source plane $p_e(x_0, y_0, z_0)$ can be obtained as [4, 21, 22, 23]

$$p_e(x_0, y_0, z_0) = \mathcal{F}^{-1} [\mathcal{F}(p_m(x_h, y_h, z_h)) \mathcal{F}(G_D(x_h - x_0, y_h - y_0, z_h - z_0))] \quad (5)$$

where \mathcal{F} and \mathcal{F}^{-1} are respectively spatial Fourier and inverse spatial Fourier transforms. The transfer function of the planar half-space Dirichlet problem is given by [24]

$$G_D(x_h - x_0, y_h - y_0, z_h - z_0) = \frac{z_h}{2\pi} \frac{(1 - ik_f r) e^{ik_f r}}{r^3} \quad (6)$$

where r is the distance between points on the hologram plane and points on the source plane and k_f is the acoustic wavenumber. A tapered cosine window (Tukey window) is suggested to reduce the effect of the unwanted high wavenumber components [23].

Based on the supersonic acoustic intensity proposed by Williams [12, 13] and the convolution theorem, Fernandez-Grande et al. [14] developed a method to calculate the supersonic intensity (SSI) using the convolution between the acoustic field and a spatial filter as follows

$$p^s(k_f, \mathbf{x}_e) = p_e(\mathbf{x}_s) * h^s(k_f, r_s(\mathbf{x}_s, \mathbf{x}_e)) \quad (7)$$

$$v^s(k_f, \mathbf{x}_e) = v_e(\mathbf{x}_s) * h^s(k_f, r_s(\mathbf{x}_s, \mathbf{x}_e)) \quad (8)$$

where $*$ denotes the convolution function, p_e is the experimental acoustic pressure, v_e is the experimental particle velocity and p^s , v^s are the supersonic components of the sound pressure and the particle velocity, respectively. $h^s(k_f, r_s(\mathbf{x}_s, \mathbf{x}_e))$ is a spatial filter proportional to the first order Bessel function of the surface distance and the acoustic wavenumber and is given by

$$h^s(k_f, r_s(\mathbf{x}_s, \mathbf{x}_e)) = \frac{k_f}{2\pi r_s(\mathbf{x}_s, \mathbf{x}_e)} J_1(k_f r_s(\mathbf{x}_s, \mathbf{x}_e)) \quad (9)$$

J_1 is the Bessel function of the first kind. \mathbf{x}_s and \mathbf{x}_e are respectively position vectors of two points on the surface and $r_s(\mathbf{x}_s, \mathbf{x}_e)$ is the surface distance between these two points. To compute the spatial radiation filter, the shortest surface distance between two arbitrary surface points on a discretized surface is calculated using the geodesic distance method [25]. The supersonic intensity (SSI) is then obtained by [14]

$$I^{\text{SSI}}(k_f, \mathbf{x}_e) = \frac{1}{2} \Re\{p^s(k_f, \mathbf{x}_e) v^s(k_f, \mathbf{x}_e)^*\} \quad (10)$$

4. Experimental and Numerical Results

An example of a point driven aluminum plate is used to compare the results from the numerical and experimental methods. The dimensions of the plate are 0.5 m \times 0.3 m. The plate is 1.5 mm thick with all four sides fixed at the boundaries. The fluid-structure is simulated in a fully coupled finite element/boundary element model. The structure is modelled using 544 8-node quadratic elements, while the fluid domain is modelled using 4-node super-parametric discontinuous linear boundary elements. Density of $\rho = 1.3 \text{ kg/m}^3$ and speed of sound of $c = 340 \text{ m/s}$ are assumed for air. Damping exists in the form of radiation damping only. A numerical modal analysis for the plate was initially conducted. A fast Fourier transform (FFT) was employed to transform the signal from the time domain to the frequency spectrum to study the modal content of the response. The natural frequencies and mode shapes from the numerical model are compared with experimental results by comparing results at the same mode shapes. A harmonic analysis using point force excitation near the corner of the plate ($x = -0.2 \text{ m}$, $y = -0.1 \text{ m}$) was then conducted to compute the sound pressure, particle velocity, active intensity and the non-negative intensity for different modes.

An experimental study was conducted to compare results for the sound pressure, normal velocity and active intensity with the results obtained numerically. The experimental set-up was placed in an anechoic chamber with volume of approximately 10 m^3 , as shown in Figure 1(a). The plate in the experimental study had the same dimensions as the plate in the numerical simulation. The plate was fixed at its

boundaries and was driven with a harmonic point force using a B&K electrodynamic shaker Type 4809 near the corner of the plate, as shown in Figure 1(b). An 8 by 8 microphone array with a spacing of 25 mm between each microphone was used to measure the sound pressure 5 mm above the plate surface. The sound pressure on the surface of the plate was then calculated based on an iterative inversion technique [24]. The normal vibration velocity of the plate was measured using a Polytec laser vibrometer OFV 505 over a grid of 20×12 positions.

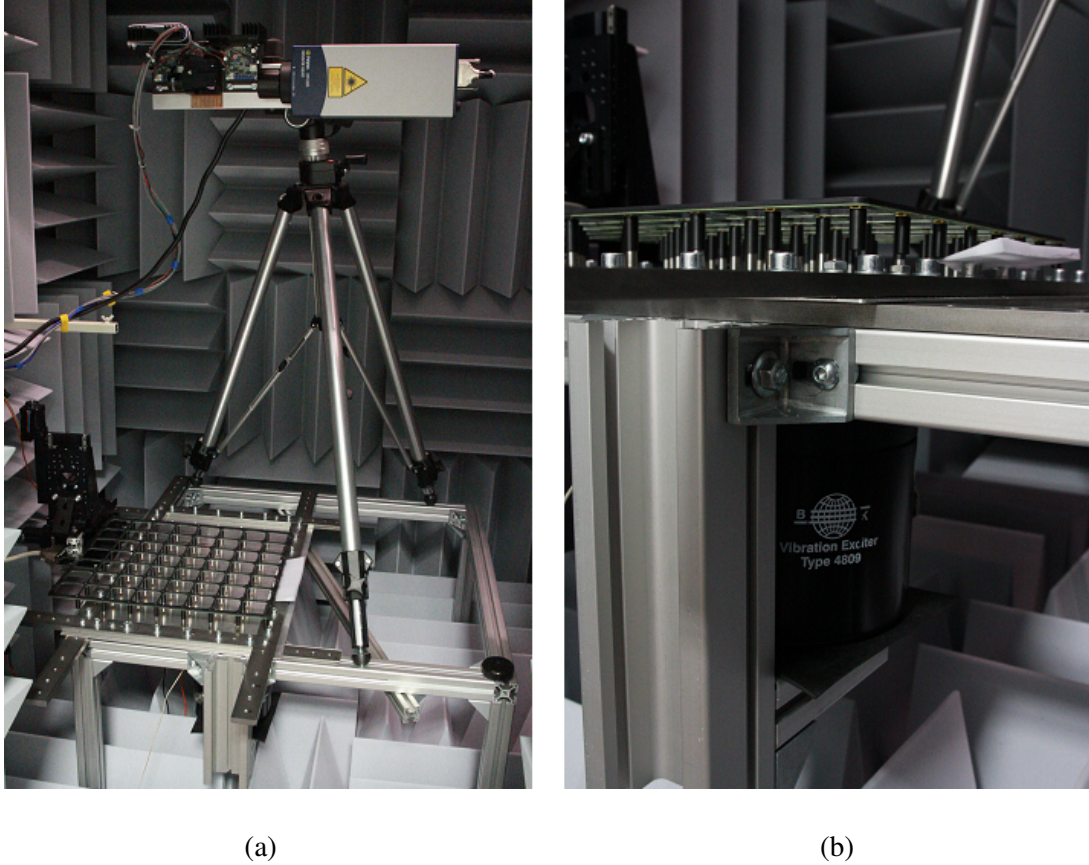


Figure 1 – (a) Experiment set-up for the rectangular aluminum plate; (b) shaker used to drive the plate.

Figures 2 and 3 compare results for the sound pressure obtained experimentally and numerically for the 1×1 and 0×3 modes, respectively. In both figures, the real part, the imaginary part and the amplitude of the experimentally predicted sound pressure on the surface of the plate obtained from the sound pressure measured on the hologram plane are presented. The sound pressures obtained numerically from a fully coupled finite element/boundary element model of the plate are also presented. The sound pressures obtained experimentally and numerically are in good agreement for both modes.

Figures 4 and 5 compare results for the normal velocity of the plate obtained experimentally and numerically for the 1×1 and 0×3 modes, respectively. In both figures, the real part, the imaginary part and the amplitude of the normal velocity on the surface of the plate are presented. The normal velocities obtained experimentally and numerically are in good agreement for both modes.

Based on the experimental and numerical results of the sound pressure and normal velocity on the plate surface, the active intensity was calculated using Eq. (1). For both modes, the amplitude of the active intensity calculated experimentally is shown as the first column of Figure 6, and similarly, the active intensity obtained numerically is shown as the second column of Figure 6. For the 0×3 mode, the active intensity results show very similar radiation patterns. For the 1×1 mode, the active intensity obtained numerically shows that the maximum radiation energy is close to the excitation location while the other three areas radiate less energy, which is slightly different from the radiation pattern of the active intensity obtained experimentally. The third and fourth columns of Figure 6 present the supersonic acoustic intensity as per Eq. (10) and the non-negative intensity as per Eq. (4). At each mode, both supersonic intensity (SSI) and non-negative intensity (NNI) exhibit different radiation patterns from the active intensity results. For the 1×1 mode, the intensity distribution patterns based on SSI and NNI are

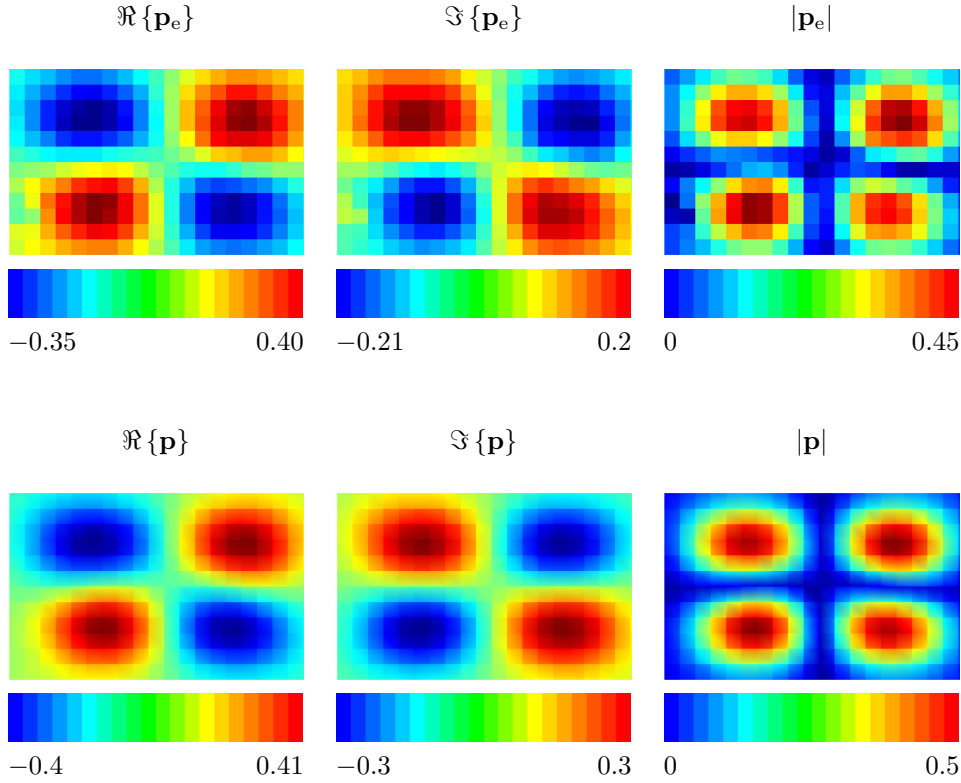


Figure 2 – The real part, the imaginary part and the amplitude of the sound pressure predicted experimentally (top) and numerically (bottom) for 1×1 mode (pressure in Pa).

in good agreement, showing the corners of the plate radiating sound. The plate corner radiation is due to cancellation of acoustic energy between adjacent areas, as previously reported [18, 26]. For the 0×3 mode, both SSI and NNI show similar radiation patterns, whereby the area close to the shorter sides of the plate are radiating sound.

5. Conclusions

Near-field acoustic holography (NAH) and non-negative intensity are used to identify the locations (hot spots) on the surface of a vibrating structure that significantly contribute to radiated noise. Based on NAH measurements, the supersonic acoustic intensity was calculated using a direct convolution between a spatial radiation filter and the acoustic pressure and normal velocity measured experimentally on the plate surface. The non-negative intensity was numerically calculated using the boundary element method. A point driven aluminum plate with fixed boundaries was examined. Two modes were selected to compare results from these two source localization techniques. Results from both techniques yield similar results and are successful in predicting sound radiation patterns from vibrating structures.

References

- [1] Koopmann, G.H. and Fahnlne, J.B., *Designing Quiet Structures*, London: Academic Press, 1997, chap. 7 - Active control of radiated acoustic power, 179–200.
- [2] Marburg, S., “Developments in structural-acoustic optimization for passive noise control”, English, *Archives of Computational Methods in Engineering* 9(4) (2002), 291–370.
- [3] Merz, S., Kessissoglou, N., Kinns, R. and Marburg, S., “Passive and active control of the radiated sound power from a submarine excited by propeller forces”, *Journal of Ship Research* 57(1) (2013), 59–71.
- [4] Williams, E.G., Maynard, J.D. and Skudrzyk, E., “Sound source reconstructions using a microphone array”, *Journal of the Acoustical Society of America* 68(1) (1980), 340–344.
- [5] Veronesi, W.A. and Maynard, J.D., “Digital holographic reconstruction of sources with arbitrarily shaped surfaces”, *Journal of the Acoustical Society of America* 85(2) (1989), 588–598.

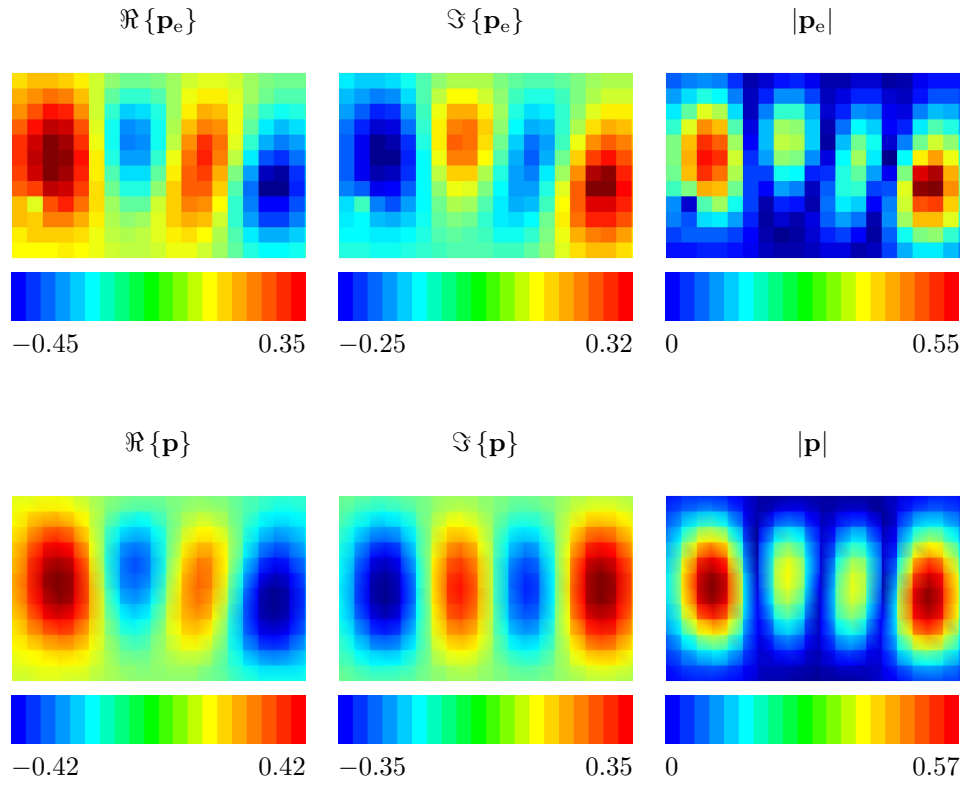


Figure 3 – The real part, the imaginary part and the amplitude of the sound pressure predicted experimentally (top) and numerically (bottom) for 0×3 mode (pressure in Pa).

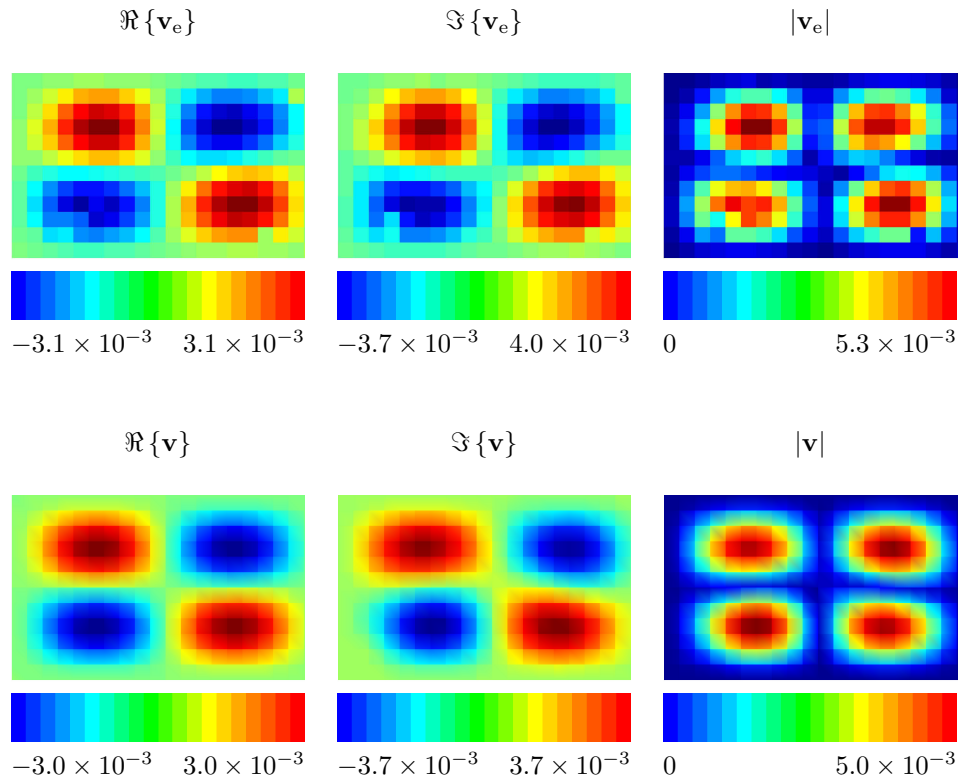


Figure 4 – The real part, the imaginary part and the amplitude of the normal velocity obtained experimentally (top) and numerically (bottom) for 1×1 mode (velocity in m/s).

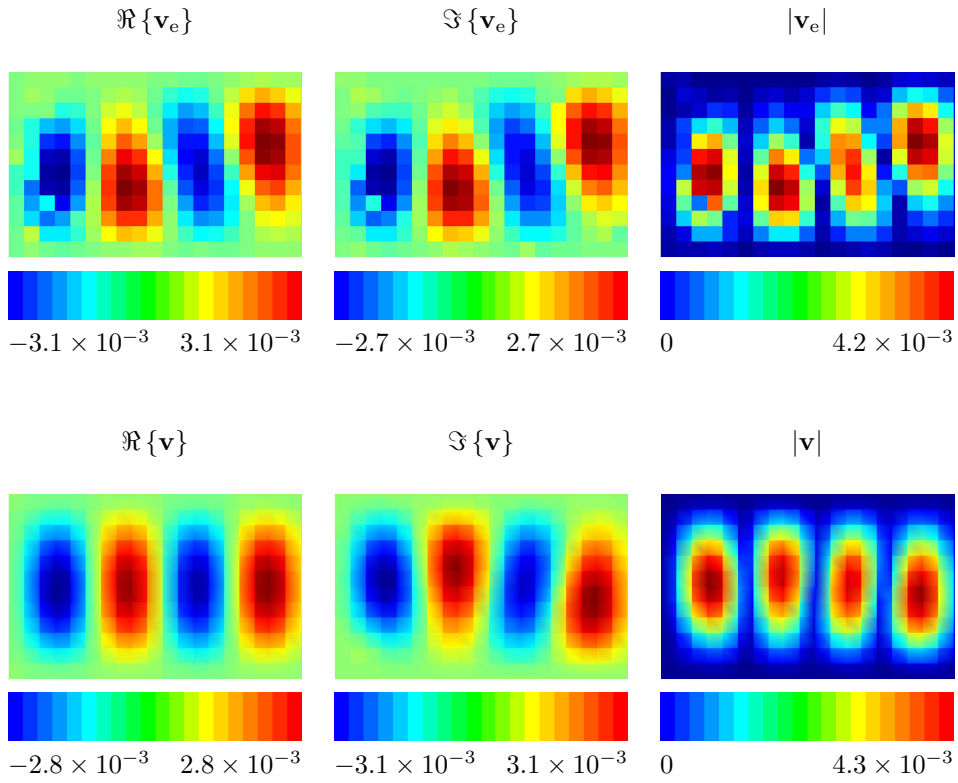


Figure 5 – The real part, the imaginary part and the amplitude of the normal velocity obtained experimentally (top) and numerically (bottom) for 0×3 mode (velocity in m/s).

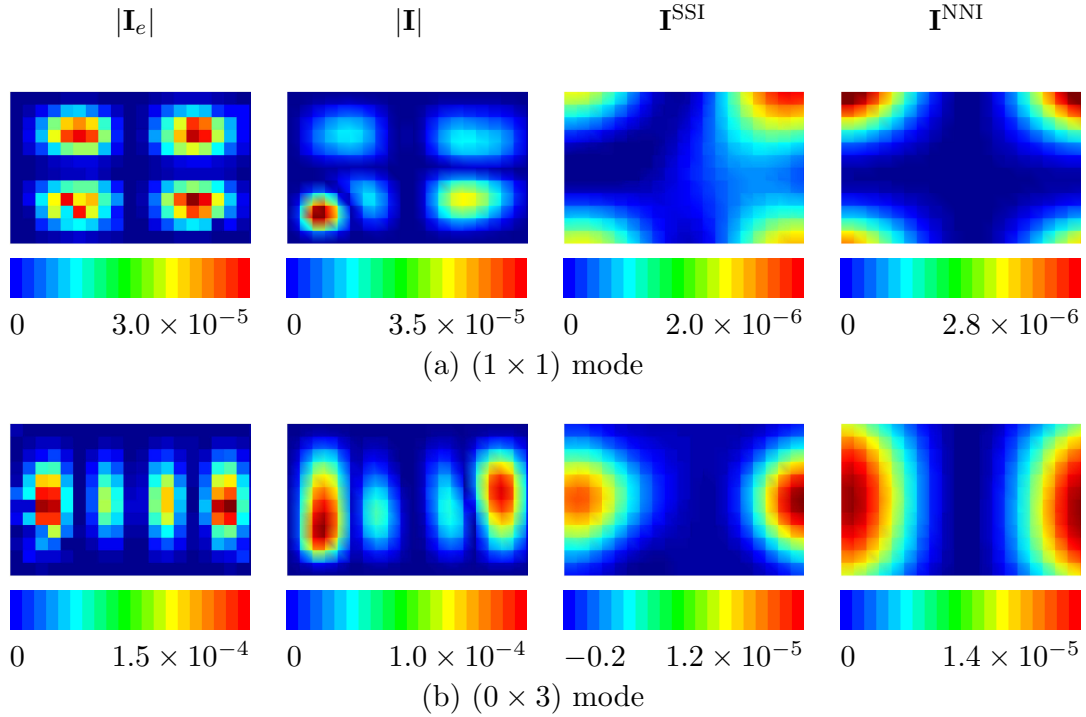


Figure 6 – Experimental acoustic intensity, numerical acoustic intensity, supersonic intensity and non-negative intensity for both 1×1 and 0×3 modes (intensity in W/m^2).

- [6] Borgiotti, G.V., Sarkissian, A., Williams, E.G. and Schuetz, L., “Conformal generalized near-field acoustic holography for axisymmetric geometries”, *Journal of the Acoustical Society of America* 88(1) (1990), 199–209.
- [7] Bai, M.R., “Application of BEM (boundary element method)-based acoustic holography to radiation analysis of sound sources with arbitrarily shaped geometries”, *Journal of the Acoustical Society of America* 92(1) (1992), 533–549.
- [8] Saijyou, K. and Yoshikawa, S., “Reduction methods of the reconstruction error for large-scale implementation of near-field acoustical holography”, *Journal of the Acoustical Society of America* 110(4) (2001), 2007–2023.
- [9] Williams, E.G., Houston, B.H. and Herdic, P.C., “Fast Fourier transform and singular value decomposition formulations for patch nearfield acoustical holography”, *Journal of the Acoustical Society of America* 114(3) (2003), 1322–1333.
- [10] Sarkissian, A., “Extension of measurement surface in near-field acoustic holography”, *Journal of the Acoustical Society of America* 115(4) (2004), 1593–1596.
- [11] Sarkissian, A., “Method of superposition applied to patch near-field acoustic holography”, *Journal of the Acoustical Society of America* 118(2) (2005), 671–678.
- [12] Williams, E.G., “Supersonic acoustic intensity”, *Journal of the Acoustical Society of America* 97(1) (1995), 121–127.
- [13] Williams, E.G., “Supersonic acoustic intensity on planar sources”, *Journal of the Acoustical Society of America* 104(5) (1998), 2845–2850.
- [14] Fernandez-Grande, E., Jacobsen, F. and Leclère, Q., “Direct formulation of the supersonic acoustic intensity in space domain”, *Journal of the Acoustical Society of America* 131(1) (2012), 186–193.
- [15] Fernandez-Grande, E. and Jacobsen, F., “Conservation of power of the supersonic acoustic intensity”, *Journal of the Acoustical Society of America* 136(2) (2014), 461–465.
- [16] Magalhães, M.B.S. and Tenenbaum, R.A., “Supersonic acoustic intensity for arbitrarily shaped sources”, *Acta Acustica united with Acustica* 92 (2006), 189–201.
- [17] Corrêa Junior, C.A. and Tenenbaum, R.A., “Useful intensity: A technique to identify radiating regions on arbitrarily shaped surfaces”, *Journal of Sound and Vibration* 332(6) (2013), 1567–1584.
- [18] Marburg, S., Lösche, E., Peters, H. and Kessissoglou, N., “Surface contributions to radiated sound power”, *Journal of the Acoustical Society of America* 133(6) (2013), 3700–3705.
- [19] Williams, E.G., “Convolution formulations for non-negative intensity”, *Journal of the Acoustical Society of America* 134(2) (2013), 1055–1066.
- [20] Marburg, S. and Nolte, B., “Computational acoustics of noise propagation in fluids - finite and boundary element methods”, Berlin, Heidelberg: Springer-Verlag, 2008, chap. 0 - A unified approach to finite and boundary element discretization in linear time-harmonic acoustics, 1–34.
- [21] Maynard, J. D., Williams, E. G. and Lee, Y., “Nearfield acoustic holography: I. Theory of generalized holography and the development of NAH”, *Journal of the Acoustical Society of America* 78(4) (1985), 1395–1413.
- [22] Williams, E. G., “Fourier acoustics : sound radiation and nearfield acoustical holography”, San Diego: Academic Press, 1999.
- [23] Havránek, Z. and Jacobsen, F., “Near field acoustic holography with double layer array processing”, *Proceedings of Euronoise 2006*, Tampere, Finland, 30 May - 1 June 2006.
- [24] Bai, M.R., “Acoustical source characterization by using recursive Wiener filtering”, *Journal of the Acoustical Society of America* 97(5) (1995), 2657–2663.
- [25] Peyré, G., Pechaud, M., Keriven, R. and Cohen, L.D., “Geodesic methods in computer vision and graphics”, *Foundations and Trends in Computer Graphics and Vision* 5(3-4) (2010), 197–397.
- [26] Maidanik, G., “Response of ribbed panels to reverberant acoustic fields”, *Journal of the Acoustical Society of America* 34(6) (1962), 809–826.